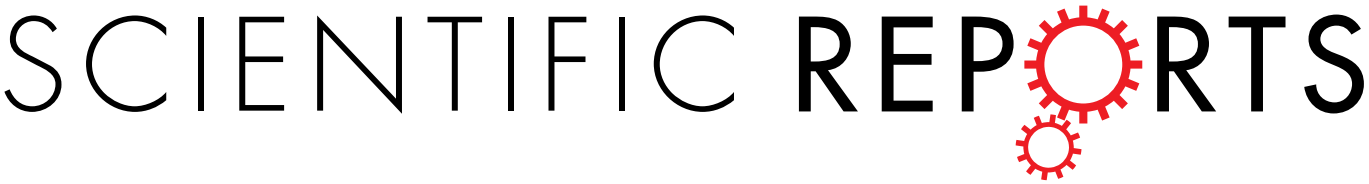

OPEN

Received: 16 May 2016
Accepted: 24 June 2016
Published: 15 July 2016

Secondary coordination sphere accelerates hole transfer for enhanced hydrogen photogeneration from [FeFe]-hydrogenase mimic and CdSe QDs in water

Min Wen, Xu-Bing Li, Jing-Xin Jian, Xu-Zhe Wang, Hao-Lin Wu, Bin Chen, Chen-Ho Tung & Li-Zhu Wu

Achieving highly efficient hydrogen (H_2) evolution *via* artificial photosynthesis is a great ambition pursued by scientists in recent decades because H_2 has high specific enthalpy of combustion and benign combustion product. [FeFe]-Hydrogenase ([FeFe]-H_2ase) mimics have been demonstrated to be promising catalysts for H_2 photoproduction. However, the efficient photocatalytic H_2 generation system, consisting of PAA-*g*-Fe_2S_2, CdSe QDs and H_2A, suffered from low stability, probably due to the hole accumulation induced photooxidation of CdSe QDs and the subsequent crash of [FeFe]-H_2ase mimics. In this work, we take advantage of supramolecular interaction for the first time to construct the secondary coordination sphere of electron donors (HA^-) to CdSe QDs. The generated secondary coordination sphere helps realize much faster hole removal with a ~30-fold increase, thus leading to higher stability and activity for H_2 evolution. The unique photocatalytic H_2 evolution system features a great increase of turnover number to 83600, which is the highest one obtained so far for photocatalytic H_2 production by using [FeFe]-H_2ase mimics as catalysts.

Nature has created [FeFe]-hydrogenase ([FeFe]-H_2ase), a type of metalloenzyme in some specific bacteria and algaes, as a H_2-forming catalyst with a high turnover rate (6000–9000 s^{-1} per catalytic site) at low over-potential[1,2]. The challenge is, however, to isolate the enzyme in large scale, and the isolated natural [FeFe]-H_2ase would lose its activity once exposure to air[3,4]. To develop effective catalysts for H_2 evolution, which is considered to be an extremely clean and renewable fuel to deal with energy crisis and environmental pollution[5–9], scientists have devoted considerable efforts to simulating the active site of [FeFe]-H_2ase[10–12]. Since the first attempt to fabricate artificial [FeFe]-H_2ase based photosynthetic system[13], [FeFe]-H_2ase mimics have been demonstrated to be a category of cost-effective and efficient catalysts for H_2 evolution under visible-light irradiation[14–18]. In particular, the efficiency of photocatalytic H_2 evolution has been dramatically enhanced by combining [FeFe]-H_2ase mimics with semiconductor quantum dots (QDs) in aqueous solution[14,19,20], which benefits from both the intrinsic ability for proton reduction of [FeFe]-H_2ase mimics and the advantage in light-absorbing and charge-separation of colloidal QDs[21]. In 2011, we used a water-soluble [FeFe]-H_2ase mimic as catalyst, CdTe QDs as photosensitizer and ascorbic acid (H_2A) as proton source and electron donor to construct an artificial photosynthetic system. Under the optimal condition, the turnover number (TON) of the system reached 505[22]. Whereafter, poly(acrylic acid)-based artificial [FeFe]-H_2ase (PAA-*g*-Fe_2S_2) has been intergrated with CdSe QDs in H_2A aqueous solution (pH 4.0) to achieve H_2 production, improving TON value high over 20000 under visible-light irradiation[23].

Key Laboratory of Photochemical Conversion and Optoelectronic Materials, Technical Institute of Physics and Chemistry & University of Chinese Academy of Sciences, Chinese Academy of Sciences, Beijing 100190, P. R. China. Correspondence and requests for materials should be addressed to X.-B.L. (email: lixubing@mail.ipc.ac.cn) or L.-Z.W. (email: lzwu@mail.ipc.ac.cn)

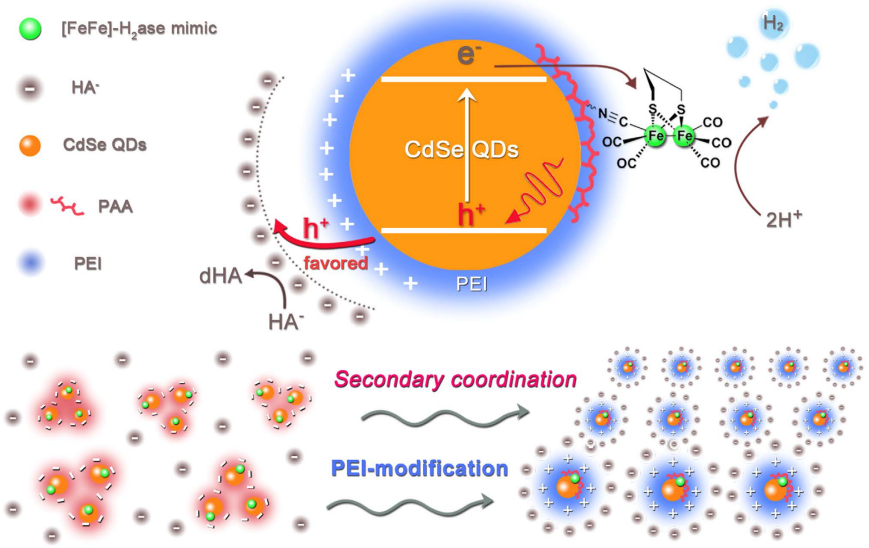

Figure 1. Schematic illustration of the secondary coordination sphere *via* PEI-modification. The dispersion of the system without (left panel) and with PEI (right panel) and the secondary coordination sphere enhanced process of photocatalytic H_2 evolution.

Nevertheless, these [FeFe]-H_2ase mimics and QDs based multi-component systems suffer from poor stability with gradual decomposion of both QDs and [FeFe]-H_2ase mimics during irradiation, which is probably due to the hole transfer rate slower than the electron transfer rate[23,24]. We found, for example, that the electron transfer rate from CdSe QDs to the active site of PAA-*g*-Fe_2S_2 is three-order faster than the hole transfer rate from CdSe QDs to H_2A[23]. In this regard, the cease of H_2 evolution might be a result of accumulating holes in the valence band of CdSe QDs. One may question whether the stability and efficiency of photocatalytic H_2 evolution system could be enhanced by means of facilitating hole removal.

In this contribution, we wish to report that the use of secondary coordination sphere greatly improves the activity and stability of the artificial [FeFe]-H_2ase-based system, consisting of CdSe QDs, PAA-*g*-Fe_2S_2 and H_2A in water (Fig. 1). Although PAA played a role in stabilizing CdSe QDs to some extent[23], the protonation of carboxylic groups under acidic condition would reduce the association of PAA with CdSe QDs[25]. Further, the negatively charged carboxyl groups would prevent CdSe QDs from negatively charged HA^- in proximity. In this situation, we envision that addition of polyethyleneimine (PEI) would be helpful for the intimate interaction of CdSe QDs with PAA-*g*-Fe_2S_2 and H_2A because PEI has the ability to protect cadmium chalcogenide nanocrystals from aggregation in an extremely wide pH range[26,27]. Unlike the most state-of-the-art approaches[28–33], we take advantage of supramolecular interaction to increase the contact between CdSe QDs and electron donors (HA^-). The positive charge of PEI under acidic condition[34] not only endows CdSe QDs a capacity to associate with PAA-*g*-Fe_2S_2 intimately, but also enables HA^- to contact closely with CdSe QDs than that in the absence of PEI. Indeed, the as-generated secondary coordination sphere helps with acceleration of hole transfer to a ~30-fold increase, while the electron transfer to PAA-*g*-Fe_2S_2 remains unchanged. As a result, the designed system can catalyze proton reduction under visible-light irradiation for 28 h, giving rise to a TON value high up to 83600. This is, to the best of our knowledge, the highest value known to date based on [FeFe]-H_2ase mimics for H_2 photogeneration.

Results

Photocatalytic H_2 generation. The H_2 evolution experiments were carried out in argon saturated aqueous solution of CdSe QDs, PAA-*g*-Fe_2S_2 and H_2A at pH 4.1 under visible-light irradiation. PAA-*g*-Fe_2S_2 and CdSe QDs were prepared according to the reported procedures[23]. The characterizations of PAA-*g*-Fe_2S_2 and CdSe QDs were described in Supplementary Information (Figs S1 and S2). As shown in Fig. 2, the photocatalytic system, containing CdSe QDs, PAA-*g*-Fe_2S_2 and H_2A at pH 4.1, ceased to evolve H_2 in 4 h, but a significant enhancement of H_2 evolution was achieved in the presence of 0.12 g·L^{-1} PEI under the same condition (Supplementary Fig. S3). Increasing the concentration of PEI to 0.46 g·L^{-1} improved the rate of H_2 production (Supplementary Fig. S4) till higher concentration to 1.84 g·L^{-1}. The excessive amount of PEI probably retarded the interaction between CdSe QDs and H_2A and/or PAA-*g*-Fe_2S_2 because the average hydrodynamic diameter of CdSe QDs remained unchanged (Supplementary Fig. S5). Note that the rate of H_2 evolution was positively proportional to the concentration of H_2A in the range of 0 to 0.1 mol·L^{-1} (Supplementary Fig. S6), and negligible H_2 was obtained in the absence of H_2A (0 mol·L^{-1}), PEI and PAA themselves were not possible to serve as electron donors in the designed system. Control experiment, performed under the same concentrations of CdSe QDs, H_2A, PAA and PEI, evolved much less H_2, which confirmed the role of Fe_2S_2 for proton reduction (Supplementary Fig. S7). To our delight, the rate of H_2 production was linear in 10 h and the lifetime of H_2 evolution could be prolonged to 28 h, yielding an unprecedented TON value to 83600 (Fig. 2).

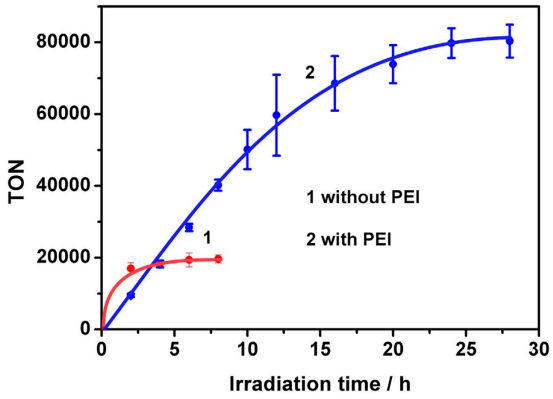

Figure 2. Photocatalytic H_2 production in the absence (line 1) and presence (line 2) of PEI. Concentrations: CdSe QDs (5.8×10^{-6} mol·L^{-1}), PAA-*g*-Fe_2S_2 (0.25 g·L^{-1}), H_2A (0.1 mol·L^{-1}), PEI (0.46 g·L^{-1}), pH 4.1.

Influence of PEI to the stability of CdSe QDs. The presence of PEI could improve the efficiency and stability of the CdSe QDs and PAA-*g*-Fe_2S_2 system for photocatalytic H_2 evolution. To verify the function of PEI, dynamic light scattering (DLS) and high-resolution transmission electron microscope (HRTEM) were employed. As shown in Fig. 3a, CdSe QDs dispersed well without any mutual aggregation under neutral condition. Upon introduction of 0.1 mol·L^{-1} H_2A (pH 4.1) to the solution, the average hydrodynamic size of CdSe QDs increased dramatically to ~1400 nm and severe aggregation of CdSe QDs was seen directly from the corresponding TEM image (Fig. 3b), a result of dissociation of surface ligands, mercaptopropionic acid (MPA), from CdSe QDs at acidic condition[35]. When a certain amount of PAA-*g*-Fe_2S_2 (0.25 g·L^{-1}) was added into the solution, the hydrodynamic size of CdSe QDs decreased from ~1400 nm to ~192 nm. The better dispersion of CdSe QDs in the presence of PAA-*g*-Fe_2S_2 was well reflected by TEM image (Fig. 3c), which provided evidence on the stabilization of PAA to CdSe QDs since there are no chemical groups in Fe_2S_2 cluster can stabilize CdSe QDs. The better dispersity of CdSe QDs caused by the coordination of PAA on the surface could also be confirmed by the enhanced emission intensity and blue-shift of band edge emission (Supplementary Fig. S8). More strikingly, when PEI (0.46 g·L^{-1}) was simultaneously introduced into the solution of CdSe QDs and PAA-*g*-Fe_2S_2, the average size distribution of CdSe QDs decreased to merely ~17 nm, which could be comparable to that in neutral water (Fig. 3d). Also, high-resolution TEM indicated the excellent dispersity of CdSe QDs in the co-presence of PAA and PEI (Fig. 3d). Clearly, the coordination between amino groups on PEI[36,37] with Cd^{2+} is so strong even under acidic condition that the presence of PEI allows an excellent dispersion of CdSe QDs at pH 4.1. The solution of the *in situ* generated PEI and PAA co-stabilized CdSe QDs was found stable for at least 7 days (Supplementary Fig. S9). The better stability of CdSe QDs in the presence of PEI ensured better interaction with PAA-*g*-Fe_2S_2, which in turn improved the efficiency and stability of this photocatalytic H_2 production system.

Consistent with the observation of HRTEM and DLS studies, an apparent blue shift of the CdSe QDs emission in the presence of PEI (Table 1 and Supplementary Fig. S8) suggested that PEI could stabilize CdSe QDs and prevent the formation of large aggregates[27]. Furthermore, with the addition of PEI (0.46 g·L^{-1}) into the solution of CdSe QDs and PAA, the emission decay was apparently facilitated from 14.7 ns to 9.6 ns (Supplementary Fig. S10). With reference to the reports in literature[38–40], the shortened lifetime could be attributed to the delocalization of photo-generated excitons, especially holes, to the surface layer of PEI, which would further benefit hole depletion of CdSe QDs by relaying holes to sacrificial reagents.

Influence of PEI to the electron transfer rate of CdSe QDs. The reductive potential of PAA-*g*-Fe_2S_2 was determined to be −0.43 V (*vs* NHE), demonstrating an exothermic electron transfer from excited CdSe QDs to PAA-*g*-Fe_2S_2 because the conduction band potential of CdSe QDs is more negative than −0.43 V (*vs* NHE)[23]. Spectroelectrochemical and time-resolved absorption spectra were then used to study the electron transfer and hole transfer process in the designed system[41–44]. Either in the absence or presence of PEI, electrochemical reduction of PAA-*g*-Fe_2S_2 led to the formation of a new absorption peak around 400 nm, which could be assigned to Fe^IFe^0 species (Supplementary Fig. S11)[45–47]. Under the same condition, electrochemical reduction of PAA and PEI couldn't result in the formation of similar signals (Supplementary Fig. S12). The results suggested that the introduction of PEI would not influence the active site of PAA-*g*-Fe_2S_2 very much. Time-resolved transient absorption spectra were measured to further evaluate the electron transfer from CdSe QDs to PAA-*g*-Fe_2S_2. As PAA-*g*-Fe_2S_2 was added into the aqueous solution of CdSe QDs, the bleaching recovery of CdSe QDs was apparently facilitated from 36.9 ns to 11.5 ns, a result of electron transfer from excited CdSe QDs to the active site of PAA-*g*-Fe_2S_2 (Fig. 4, Supplementary Table S1)[23,41]. The rate of electron transfer (k_e) was determined[41] to be 3.4×10^{11} M^{-1}·s^{-1} and 4.5×10^{11} M^{-1}·s^{-1} in the absence and presence of PEI (0.46 g·L^{-1}), respectively (Table 1, see details in Supplementary Information). Obviously, the introduction of PEI could hardly change electron transfer from CdSe QDs to PAA-*g*-Fe_2S_2 for proton reduction.

Influence of PEI to the hole transfer rate of CdSe QDs. The hole transfer kinetics from CdSe QDs to HA^- was carefully examined[42,43]. Progressive addition of ascorbate sodium (NaHA) to aqueous solutions, *i.e.* CdSe QDs and PAA; CdSe QDs, PAA and PEI, at pH 4.1, respectively, resulted in emission quenching of CdSe

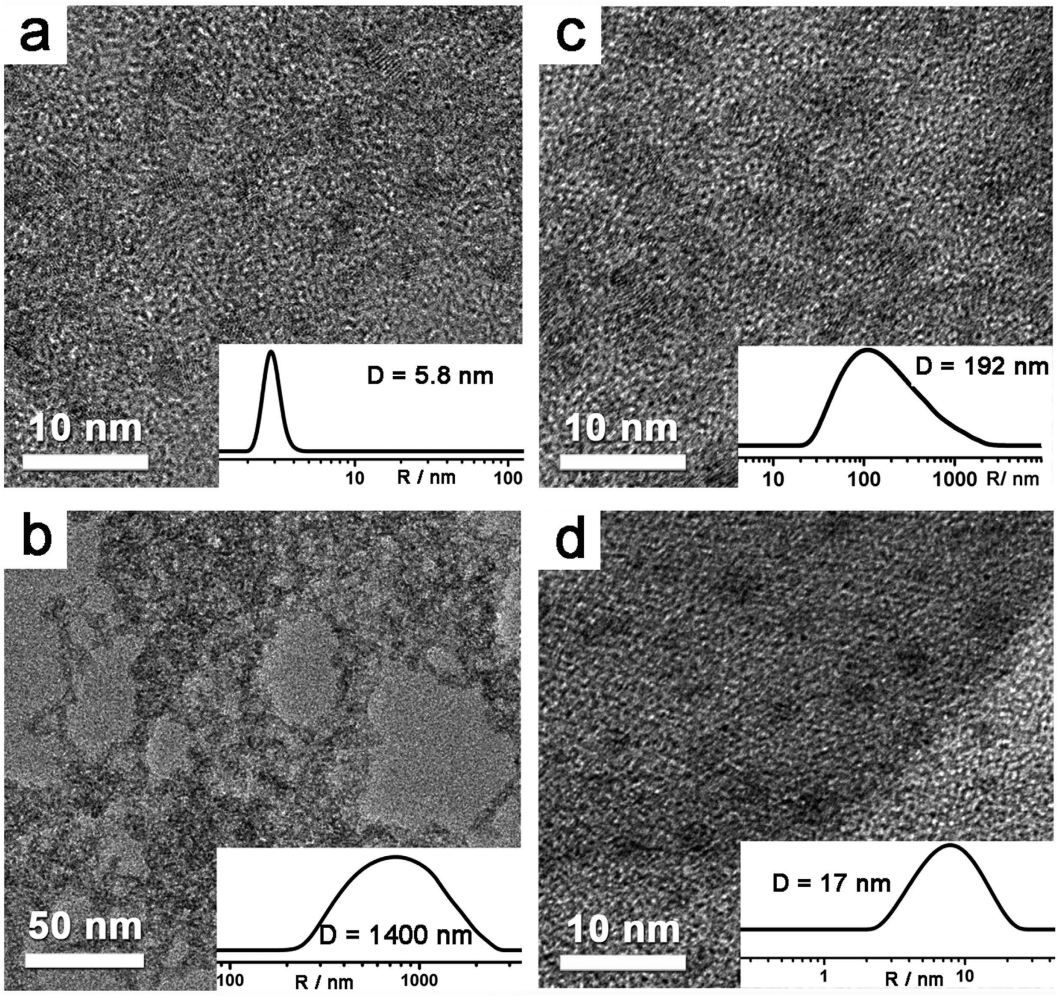

Figure 3. TEM images and corresponding DLS profiles (the inset panels) of CdSe QDs in water under different conditions. (**a**) In neutral water, pH 6.9; (**b**) in the presence of H_2A, pH 4.1; (**c**) in the presence of H_2A and PAA-*g*-Fe_2S_2, pH 4.1; (**d**) in the presence of H_2A, PAA-*g*-Fe_2S_2 and PEI, pH 4.1. Concentrations: CdSe QDs (5.8×10^{-6} mol·L^{-1}), H_2A (0.1 mol·L^{-1}), PAA-*g*-Fe_2S_2 (0.25 g·L^{-1}), PEI (0.46 g·L^{-1}).

Systems	λ_e/nm	τ_e/ns	k_e/M^{-1}·s^{-1}	k_h/M^{-1}·s^{-1}	ζ/mV	TON	$t_{lifetime}$/h
without PEI	479	14.7	3.4×10^{11}	4.6×10^{8}	−8.7	20000	4
with PEI	475	9.6	4.5×10^{11}	1.5×10^{10}	+25.7	83600	28

Table 1. Properties of systems for H_2 evolution in the presence and absence of PEI. (λ_e) Emission peak of CdSe QDs; (τ_e) Emission lifetime of CdSe QDs; (k_e) The rate of electron transfer from CdSe QDs to PAA-*g*-Fe_2S_2; (k_h) The rate of hole transfer from CdSe QDs to H_2A; (ζ) Zeta potential; (TON) Turnover number of the systems; ($t_{lifetime}$) The time that the systems could catalyze proton reduction.

QDs to varied extent. Combining with the emission decay with and without PEI (Supplementary Fig. S10), the rate of hole transfer (k_h) from CdSe QDs to HA^- was determined as 1.5×10^{10} M^{-1}·s^{-1} and 4.6×10^{8} M^{-1}·s^{-1} (Table 1, Fig. 5, Supplementary Figs S13 and S14, see details in Supplementary Information). Surprisingly, a ~30-fold enhancement of hole transfer was obtained with the addition of PEI. The presence of PEI facilitated the hole-extraction pathway of CdSe QDs by HA^-. Considering the coordination of amino groups of PEI on the surface of CdSe QDs, the superficial electric charge of CdSe QDs would be altered. Indeed, the zeta potentials (ζ) of CdSe QDs in H_2A (0.1 mol·L^{-1}) solution, and in H_2A (0.1 mol·L^{-1}) and PAA (0.25 g·L^{-1}) solution were measured to be −4.7 mV and −8.7 mV, respectively (Table 1, Supplementary Table S2). After adding PEI (0.46 g·L^{-1}) into the solution, the ζ value changed to +25.7 mV, indicating the extremely strong positive charge of PEI modified CdSe QDs. On the one hand, the strongly positive charge ensured the excellent stability of CdSe QDs in water due to the strong electrostatic repulsion, *vide ante* (Supplementary Fig. S9). On the other hand, the inversed charge of CdSe QDs surface provided a driving force to interact with negatively charged HA^- by electrostatic interaction.

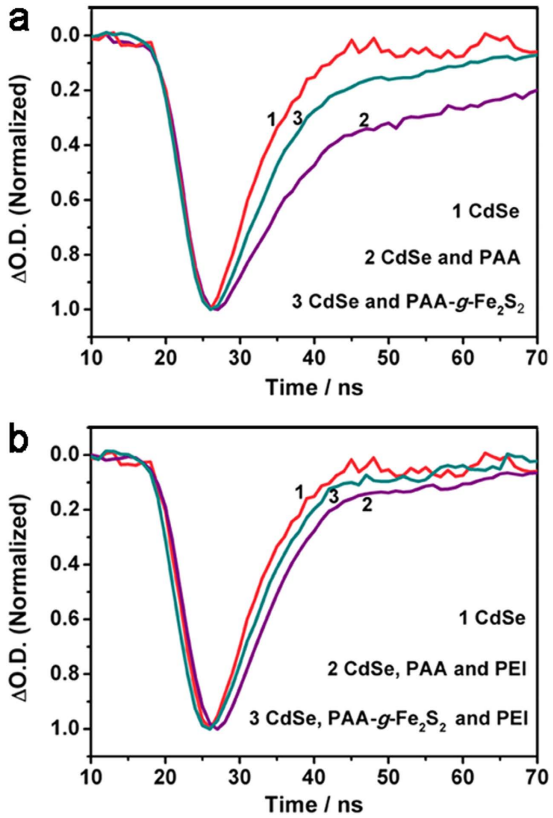

Figure 4. Transient absorption measurements. (**a**) The recovery kinetics of CdSe QDs at 430 nm in water at pH 4.1 (line 1), in the presence of PAA (line 2) and PAA-*g*-Fe_2S_2 (line 3); (**b**) the recovery kinetics of CdSe QDs at 430 nm in water at pH 4.1 (line 1), in the presence of PAA and PEI (line 2), and PAA-*g*-Fe_2S_2 and PEI (line 3). Concentrations: CdSe QDs (1.6×10^{-5} mol·L^{-1}), PAA (0.25 g·L^{-1}), PAA-*g*-Fe_2S_2 (0.25 g·L^{-1}), PEI (0.46 g·L^{-1}), pH 4.1.

The as-generated secondary coordination sphere strengthened the association of HA^- with CdSe QDs, which in turn accelerated the hole transfer from CdSe QDs to HA^-[48].

The accelerated hole transfer process is well-manifested by the model of electrical double layer (EDL) to estimate the concentration of adsorbed counterion (see details in Supplementary Information)[49]. For PAA and PEI/PAA stabilized CdSe QDs, the surface adsorbed HA^- ions were determined as 0.07 mol·L^{-1} and 0.27 mol·L^{-1}, respectively. The secondary coordination sphere of HA^- to CdSe QDs, simply by addition of PEI, contributed a ~30-fold increase of hole transfer from CdSe QDs to HA^- and a significant decrease of k_e/k_h ratio from ~740 to ~30, which benefited the balance of excitons consumption and protected CdSe QDs from photo-oxidation during visible-light irradiation. As a result, the CdSe QDs and PAA-*g*-Fe_2S_2 system that would decompose in 4 h irradiation showed a remarkably enhanced activity and stability for photocatalytic H_2 evolution.

Discussion

On the basis of above results, we speculated that the secondary coordination sphere is crucial for the enhancement of H_2 photogeneration from [FeFe]-H_2ase mimic and CdSe QDs in water. Upon photoexcitation, CdSe QDs induces electrons promoting to the conduction band and leaving holes in the valence band to form separated electron/hole pairs. Photoexcited electron in the conduction band of CdSe QDs transfers to the Fe_2S_2 core of PAA-*g*-Fe_2S_2 and generates a one-electron reduced Fe^IFe^0 species. This active species further reacts with a proton in catalytic cycle to produce H_2. At the same time, the leaving hole in the valence band of CdSe QDs is captured by electron donor HA^- to regenerate CdSe QDs. Because two electrons are required to produce each molecular H_2, the regeneration of both CdSe QDs and Fe_2S_2 active site of [FeFe]-H_2ase mimic is imperative. So the better balance of electron transfer and hole transfer of CdSe QDs to PAA-*g*-Fe_2S_2 and HA^- is, the higher efficiency of H_2 evolution would be. In this typical PAA-*g*-Fe_2S_2-based system, the *in situ* PEI-modification can greatly improve the stability of CdSe QDs to a well-dispersed colloidal solution under acidic condition (Fig. 1), which ensures smooth electron transfer from CdSe QDs to PAA-*g*-Fe_2S_2. More importantly, the *in situ* PEI modification induces the secondary coordination of negatively charged sacrificial reagents (HA^-) to the positively charged surface of the modified CdSe QDs, which contributes a 30-fold enhancement of hole transfer rate. Benefitting from these advantages, the photocorrosion of CdSe QDs is avoided to a great extent by facilitating hole extraction, and thus greatly enhancing the efficiency and stability of CdSe QDs and PAA-*g*-Fe_2S_2 system for photocatalytic H_2 evolution.

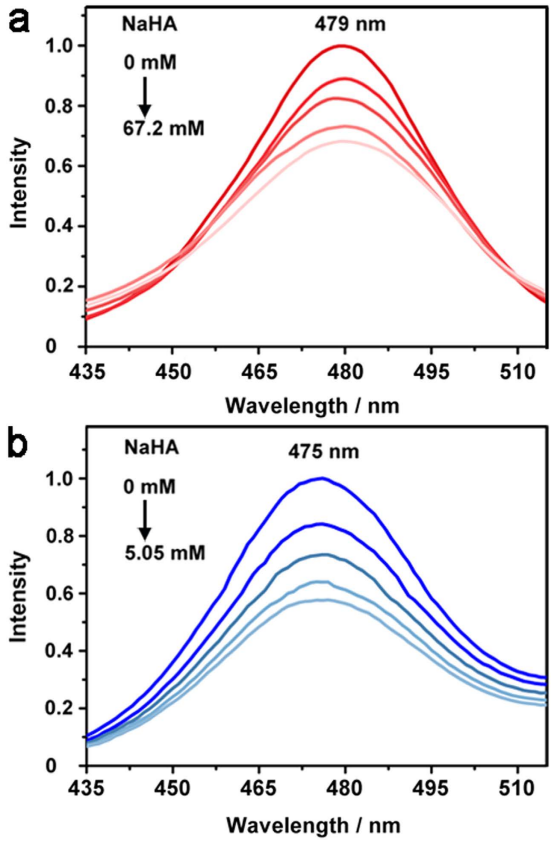

Figure 5. Hole depletion of CdSe QDs. The emission quenching of CdSe QDs with gradual addition of NaHA in the presence of PAA (**a**) and in the presence of PAA and PEI (**b**). Concentrations: CdSe QDs (1.6×10^{-5} mol·L^{-1}), PAA (0.25 g·L^{-1}), PAA-*g*-Fe_2S_2 (0.25 g·L^{-1}), PEI (0.46 g·L^{-1}), pH 4.1.

In summary, we have demonstrated for the first time that secondary coordination sphere enables to facilitate hole transfer for efficient H_2 photogeneration. In terms of supramolecular interaction, the performance of photocatalytic system, *i.e.* CdSe QDs, PAA-*g*-Fe_2S_2, and H_2A at pH 4.1, has been improved by PEI to 83600 turnovers, which is the highest value known to date for photocatalytic H_2 evolution by using [FeFe]-H_2ase mimics as catalysts. Studies on steady-state and time-resolved spectroscopy reveal that the presence of PEI greatly enhances the rate of hole transfer up to ~30-fold as compared with the same system without PEI. As a result, the ratio (k_e/k_h) of electron transfer and hole transfer from CdSe QDs to PAA-*g*-Fe_2S_2 and HA^- decreases from 740 to 30, which is advantageous to the balance of excitons generated by photoexcited CdSe QDs to synergistically improve the efficiency of H_2 evolution. Our results imply that environment surrounding each component, for example, CdSe QDs photosensitizer, Fe_2S_2 catalyst and H_2A sacrifical electron donor and proton source in this case, might cause significant activity difference of photocatalytic system. The crucial role of PEI suggests that to create efficient H_2 evolution systems based on [FeFe]-H_2ase mimic, one would need to mimic not only the active site structure of [FeFe]-H_2ase but also the kinetic balance for electron transfer and hole transfer in a real H_2 evolution system. It is anticipated that the use of secondary coordination sphere would be a promising alternative to enhance the stability and efficiency of artifical [FeFe]-H_2ase-based system for H_2 evolution, which is reminiscent of natural [FeFe]-H_2ase buried in protein matrix.

Methods

H_2 evolution experiments. A typical procedure for H_2 production was described as follows. Certain amounts of PAA-*g*-Fe_2S_2, MPA-CdSe QDs, H_2A and PEI were dissolved in ultrapure water respectively, to make a solution at certain concentration. Then, certain volumes of the solutions for PAA-*g*-Fe_2S_2, MPA-CdSe QDs, H_2A and PEI were taken to mix in a Schlenk tube. The pH value of the solutions were determined by a pH meter and adjusted by aqueous NaOH or HCl solution. The total volume of the mixed solution was diluted with ultrapure water to 5 mL. Thereafter, the sample was saturated with argon gas and 1000 μL CH_4 was injected as the internal standard for quantitative GC-TCD analysis. The light source was a blue LED lamp (3 W, $\lambda = 450$ nm) equipped with an agitator and a cooling apparatus. After a certain period of irradiation time, 500 μL mixed gas was taken from the sample tube and injected into the GC for analysis. The response factor for H_2 was 8.47 and the response factor for CH_4 was 2.09 under the experimental condition, which were established by calibration with known amounts of H_2 and CH_4, and determined before and after a series of measurements.

Synthesis of MPA-CdSe QDs. MPA-CdSe QDs were synthesized according to the literature with slight modification[50]. Briefly, selenium powder (40 mg) was added into Na_2SO_3 aqueous solution (100 mL, 1.5 mmol). The mixture was refluxed at 130 degree until the solid powder of selenium disappeared and then colourless transparent Na_2SeSO_3 solution was obtained. The Na_2SeSO_3 solution (10 mL) was extracted and injected into the argon saturated $CdCl_2$ solution (46 mg $CdCl_2{\cdot}2.5H_2O$ in 190 mL ultrapure water) at pH 11 in the presence of 3-mercaptopropionic acid (26 uL) as stabilizing agent. The resulting mixture was refluxed at 120 degree to control the growth of CdSe QDs. The size of QDs was monitored by UV-vis absorption spectrum during refluxing.

Synthesis of PAA-*g*-Fe_2S_2. The water soluble catalyst PAA-*g*-Fe_2S_2 was synthesized according to our previous procedure[23]. The color of pure PAA is white and the color of pure Fe_2S_2 active site is red. After modification, the color of PAA changed from white to light red, indicating the successful anchor of Fe_2S_2 on the chain of PAA. ^{1}H-NMR, UV/Vis spectrum and FTIR spectroscopy further confirmed the modification of the Fe_2S_2 active site onto the chain of PAA. The grafting amount of Fe_2S_2 was determined as 2.8×10^{-6} mol·g^{-1} for PAA-*g*-Fe_2S_2 by inductively coupled plasma-atomic emission spectrometry (ICP-AES) based on the relative content of Fe in samples. Spectroelectrochemical and time-resolved absorption spectra experiments employed PAA-*g*-Fe_2S_2 with larger grafting amount of Fe_2S_2 site (7.1×10^{-4} mol·g^{-1}) as electron capture to obtain more obvious signals.

Details of the instruments, chemicals and the computing methods used in this work are given in the Supplementary Information.

References

1. Lubitz, W., Ogata, H., Rudiger, O. & Reijerse, E. Hydrogenases. *Chem. Rev.* **114,** 4081–4148 (2014).
2. Hemschemeier, A., Melis, A. & Happe, T. Analytical approaches to photobiological hydrogen production in unicellular green algae. *Photosynth. Res.* **102,** 523–540 (2009).
3. Lambertz, C. *et al.* O_2 reactions at the six-iron active site (H-cluster) in [FeFe]-hydrogenase. *J. Biol. Chem.* **286,** 40614–40623 (2011).
4. Swanson, K. D. *et al.* [FeFe]-Hydrogenase Oxygen Inactivation Is Initiated at the H Cluster 2Fe Subcluster. *J. Am. Chem. Soc.* **137,** 1809–1816 (2015).
5. Esswein, A. J. & Nocera, D. G. Hydrogen Production by Molecular Photocatalysis. *Chem. Rev.* **107,** 4022–4047 (2007).
6. Ran, J., Zhang, J., Yu, J., Jaroniec, M. & Qiao, S. Z. Earth-abundant cocatalysts for semiconductor-based photocatalytic water splitting. *Chem. Soc. Rev.* **43,** 7787–7812 (2014).
7. Singh, W. M. *et al.* Electrocatalytic and photocatalytic hydrogen production in aqueous solution by a molecular cobalt complex. *Angew. Chem. Int. Ed.* **51,** 5941–5944 (2012).
8. Zhang, J., Chen, Y. & Wang, X. Two-dimensional covalent carbon nitride nanosheets: synthesis, functionalization, and applications. *Energy Environ. Sci.* **8,** 3092–3108 (2015).
9. Han, Z., Qiu, F., Eisenberg, R., Holland, P. L. & Krauss, T. D. Robust Photogeneration of H_2 in Water Using Semiconductor Nanocrystals and a Nickel Catalyst. *Science* **338,** 1321–1324 (2012).
10. Tard, C. & Pickett, C. J. Structural and Functional Analogues of the Active Sites of the [Fe]-, [NiFe]-, and [FeFe]-Hydrogenases. *Chem. Rev.* **109,** 2245–2274 (2009).
11. Li, Y., Zhong, W., Qian, G. F., Xiao, Z. Y. & Liu, X. M. Using polyethyleneimine (PEI) as a scaffold to construct mimicking systems of [FeFe]-hydrogenase: preparation, characterization of PEI-based materials, and their catalysis on proton reduction. *Appl. Organomet. Chem.* **27,** 253–260 (2013).
12. Qian, G. *et al.* Diiron hexacarbonyl complexes bearing naphthalene-1,8-dithiolate bridge moiety as mimics of the sub-unit of [FeFe]-hydrogenase: synthesis, characterisation and electrochemical investigations. *New. J. Chem.* **39,** 9752–9760 (2015).
13. Ott, S., Kritikos, M., Akermark, B. & Sun, L. C. Synthesis and structure of a biomimetic model of the iron hydrogenase active site covalently linked to a ruthenium photosensitizer. *Angew. Chem. Int. Ed.* **42,** 3285–3288 (2003).
14. Wu, L.-Z., Chen, B., Li, Z.-J. & Tung, C.-H. Enhancement of the efficiency of photocatalytic reduction of protons to hydrogen via molecular assembly. *Acc. Chem. Res.* **47,** 2177–2185 (2014).
15. Wang, F. *et al.* Artificial Photosynthetic Systems Based on [FeFe]-Hydrogenase Mimics: the Road to High Efficiency for Light-Driven Hydrogen Evolution. *ACS Catal.* **2,** 407–416 (2012).
16. Simmons, T. R., Berggren, G., Bacchi, M., Fontecave, M. & Artero, V. Mimicking hydrogenases: From biomimetics to artificial enzymes. *Coord. Chem. Rev.* **270–271,** 127–150 (2014).
17. Streich, D. *et al.* High-Turnover Photochemical Hydrogen Production Catalyzed by a Model Complex of the [FeFe]-Hydrogenase Active Site. *Chem. Eur. J.* **16,** 60–63 (2010).
18. Wang, F. *et al.* Amphiphilic polymeric micelles as microreactors: improving the photocatalytic hydrogen production of the [FeFe]-hydrogenase mimic in water. *Chem. Commun.* **52,** 457–460 (2016).
19. Nann, T. *et al.* Water splitting by visible light: a nanophotocathode for hydrogen production. *Angew. Chem. Int. Ed.* **49,** 1574–1577 (2010).
20. Wen, F. *et al.* A hybrid photocatalytic system comprising ZnS as light harvester and an [Fe(2)S(2)] hydrogenase mimic as hydrogen evolution catalyst. *ChemSusChem* **5,** 849–853 (2012).
21. Smith, A. M. & Nie, S. Semiconductor Nanocrystals: Structure, Properties, and Band Gap Engineering. *Acc. Chem. Res.* **43,** 190–200 (2010).
22. Wang, F. *et al.* A Highly Efficient Photocatalytic System for Hydrogen Production by a Robust Hydrogenase Mimic in an Aqueous Solution. *Angew. Chem. Int. Ed.* **50,** 3193–3197 (2011).
23. Wang, F. *et al.* Exceptional Poly(acrylic acid)-Based Artificial [FeFe]-Hydrogenases for Photocatalytic H_2 Production in Water. *Angew. Chem. Int. Ed.* **52,** 8134–8138 (2013).
24. Knowles, K. E., Peterson, M. D., McPhail, M. R. & Weiss, E. A. Exciton Dissociation within Quantum Dot–Organic Complexes: Mechanisms, Use as a Probe of Interfacial Structure, and Applications. *J. Phys. Chem. C* **117,** 10229–10243 (2013).
25. Choi, J. & Rubner, M. F. Influence of the Degree of Ionization on Weak Polyelectrolyte Multilayer Assembly. *Macromolecules* **38,** 116–124 (2005).
26. Zhuang, Z., Lu, X., Peng, Q. & Li, Y. Direct Synthesis of Water-Soluble Ultrathin CdS Nanorods and Reversible Tuning of the Solubility by Alkalinity. *J. Am. Chem. Soc.* **132,** 1819–1821 (2010).
27. Liang, W.-J. *et al.* Branched polyethylenimine improves hydrogen photoproduction from a CdSe quantum dot/[FeFe]-hydrogenase mimic system in neutral aqueous solutions. *Chem. Eur. J.* **21,** 3187–3192 (2015).
28. Li, X.-B. *et al.* Hole-Accepting-Ligand-Modified CdSe QDs for Dramatic Enhancement of Photocatalytic and Photoelectrochemical Hydrogen Evolution by Solar Energy. *Adv. Sci.* **3,** 1500282 (2016).
29. Bi, W. *et al.* Molecular co-catalyst accelerating hole transfer for enhanced photocatalytic H_2 evolution. *Nat. Commun.* **6,** 8647 (2015).
30. Song, N., Zhu, H., Jin, S. & Lian, T. Hole Transfer from Single Quantum Dots. *ACS Nano* **5,** 8750–8759 (2011).
31. Tarafder, K., Surendranath, Y., Olshansky, J. H., Alivisatos, A. P. & Wang, L.-W. Hole Transfer Dynamics from a CdSe/CdS Quantum Rod to a Tethered Ferrocene Derivative. *J. Am. Chem. Soc.* **136,** 5121–5131 (2014).

32. Olshansky, J. H., Ding, T. X., Lee, Y. V., Leone, S. R. & Alivisatos, A. P. Hole Transfer from Photoexcited Quantum Dots: The Relationship between Driving Force and Rate. *J. Am. Chem. Soc.* **137,** 15567–15575 (2015).
33. Wu, K., Du, Y., Tang, H., Chen, Z. & Lian, T. Efficient Extraction of Trapped Holes from Colloidal CdS Nanorods. *J. Am. Chem. Soc.* **137,** 10224–10230 (2015).
34. von Harpe, A., Petersen, H., Li, Y. & Kissel, T. Characterization of commercially available and synthesized polyethylenimines for gene delivery. *J. Controlled Release* **69,** 309–322 (2000).
35. Aldana, J., Lavelle, N., Wang, Y. & Peng, X. Size-Dependent Dissociation pH of Thiolate Ligands from Cadmium Chalcogenide Nanocrystals. *J. Am. Chem. Soc.* **127,** 2496–2504 (2005).
36. Kobayashi, S., Hiroishi, K., Tokunoh, M. & Saegusa, T. Chelating properties of linear and branched poly(ethylenimines). *Macromolecules* **20,** 1496–1500 (1987).
37. Kadioglu, S. I., Yilmaz, L. & Ozbelge, H. O. Estimation of Binding Constants of Cd(II), Ni(II) and Zn(II) with Polyethyleneimine (PEI) by Polymer Enhanced Ultrafiltration (PEUF) Technique. *Sep. Sci. Technol.* **44,** 2559–2581 (2009).
38. Tamura, H. & Burghardt, I. Ultrafast Charge Separation in Organic Photovoltaics Enhanced by Charge Delocalization and Vibronically Hot Exciton Dissociation. *J. Am. Chem. Soc.* **135,** 16364–16367 (2013).
39. Che, Y. *et al.* Enhancing One-Dimensional Charge Transport through Intermolecular π-Electron Delocalization: Conductivity Improvement for Organic Nanobelts. *J. Am. Chem. Soc.* **129,** 6354–6355 (2007).
40. Heiber, M. C. & Dhinojwala, A. Estimating the Magnitude of Exciton Delocalization in Regioregular P3HT. *J. Phys. Chem. C* **117,** 21627–21634 (2013).
41. Farrow, B. & Kamat, P. V. CdSe Quantum Dot Sensitized Solar Cells. Shuttling Electrons Through Stacked Carbon Nanocups. *J. Am. Chem. Soc.* **131,** 11124–11131 (2009).
42. Tseng, H.-W., Wilker, M. B., Damrauer, N. H. & Dukovic, G. Charge Transfer Dynamics between Photoexcited CdS Nanorods and Mononuclear Ru Water-Oxidation Catalysts. *J. Am. Chem. Soc.* **135,** 3383–3386 (2013).
43. Han, Z., McNamara, W. R., Eum, M.-S., Holland, P. L. & Eisenberg, R. A Nickel Thiolate Catalyst for the Long-Lived Photocatalytic Production of Hydrogen in a Noble-Metal-Free System. *Angew. Chem. Int. Ed.* **51,** 1667–1670 (2012).
44. Baker, D. R. & Kamat, P. V. Tuning the Emission of CdSe Quantum Dots by Controlled Trap Enhancement. *Langmuir* **26,** 11272–11276 (2010).
45. Borg, S. J. *et al.* Electron transfer at a dithiolate-bridged diiron assembly: Electrocatalytic hydrogen evolution. *J. Am. Chem. Soc.* **126,** 16988–16999 (2004).
46. Samuel, A. P. S., Co, D. T., Stern, C. L. & Wasielewski, M. R. Ultrafast Photodriven Intramolecular Electron Transfer from a Zinc Porphyrin to a Readily Reduced Diiron Hydrogenase Model Complex. *J. Am. Chem. Soc.* **132,** 8813–8815 (2010).
47. Na, Y. *et al.* Visible Light-Driven Electron Transfer and Hydrogen Generation Catalyzed by Bioinspired [2Fe2S] Complexes. *Inorg. Chem.* **47,** 2805–2810 (2008).
48. Wang, Y. *et al.* Driving charge separation for hybrid solar cells: photo-induced hole transfer in conjugated copolymer and semiconductor nanoparticle assemblies. *Phys. Chem. Chem. Phys.* **16,** 5066–5070 (2014).
49. Somasundaran, P., Healy, T. W. & Fuerstenau, D. W. Surfactant Adsorption at the Solid-Liquid Interface-Dependence of Mechanism on Chain Length. *J. Phys. Chem.* **68,** 3562–3566 (1964).
50. Park, Y.-S. *et al.* Aqueous Phase Synthesized CdSe Nanoparticles with Well-Defined Numbers of Constituent Atoms. *J. Phys. Chem. C* **114,** 18834–18840 (2010).

Acknowledgements

We are grateful for financial support from the Ministry of Science and Technology of China (2013CB834505, 2014CB239402 and 2013CB834804), the National Science Foundation of China (91427303, 21390404 and 51373193), Strategic Priority Research Program of the Chinese Academy of Science (XDB17030200), and the Chinese Academy of Sciences.

Author Contributions

L.-Z.W. and X.-B.L. designed the research and supervised the whole project; M.W. performed experiments with the input from J.-X.J., X.-Z.W., H.-L.W. and B.C.; C.-H.T. helped with the discussion.

Additional Information

Supplementary information accompanies this paper at http://www.nature.com/srep

Competing financial interests: The authors declare no competing financial interests.

How to cite this article: Wen, M. *et al.* Secondary coordination sphere accelerates hole transfer for enhanced hydrogen photogeneration from [FeFe]-hydrogenase mimic and CdSe QDs in water. *Sci. Rep.* **6**, 29851; doi: 10.1038/srep29851 (2016).